Extraction of P and Scholte waves from ambient seafloor noise record observed by distributed acoustic sensing

T. Tonegawa[1], E. Araki[1], H. Matsumoto[1], T. Kimura[1], K. Obana[1], G. Fujie[1], R. Arai[1], K. Shiraishi[1], M. Nakano[1], Y. Nakamura[1], T. Yokobiki[1], and S. Kodaira[1]

[1] Japan Agency for Marine-Earth Science and Technology (JAMSTEC), 2-15, Natsushima, Yokosuka, Kanagawa, 237-0061, Japan.

Contents of this file

Introduction

Text S1 explains the numerical simulation settings. Figure S1 show the geometry among the reference point, station, and cable. Figure S2 shows the CCFs at 0.1–0.3 Hz for 10-km subarrays for Stage A. Figure S3 shows the CCFs in the frequency-wavenumber domains obtained for 5-km subarrays for Stage A. Figure S4 shows the CCFs at different parameters for the 20-km subarray. Figure S5 shows the Vs perturbation profiles along the cable. Figure S6 shows the incident angle estimation of P waves to the seafloor. Figure S7 displays the synthesized wavefield associated with a source at the sea surface. Figure S8 displays the Vs structures using the CCFs stacked for different days. Table S1 shows the reference points and frequency bands for the inversion at the 5-km subarrays.

Text S1. Numerical simulation

We conducted a 2D finite difference method with a rotated-staggered grid for second order approximations in time and space (Saenger et al. 2000). The calculation has been performed in the displacement-stress scheme with an absorbing boundary condition (Clayton and Engquist, 1977). The model space is 200×20 km^2, and the grid size is 50×50 m^2. The water depth is 1 km. We applied a vertical single force with Ricker wavelets for central (maximum) frequencies of 0.22 Hz (0.29 Hz) at x = 100 km and z = 0 km (sea surface). Stations are set at the seafloor within a distance ranging between 50–150 km with an interval of 0.5 km.

The seismic velocity structure at the subseafloor is based on the 1D *Vp* structure with a reduction (orange line in Fig. S6a). The *Vs* and density were derived from *Vp* using empirical relations (Brocher, 2005). In the sea water, *Vp*, *Vs* and density are 1.5 km/s, 0 km/s and 1.0 g/cm^3. Because the calculation was unstable in the cases where *Vp/Vs* of the accretionary prism at shallow depths was large, we set *Vp/Vs* = 3.0 when *Vp/Vs* > 3.0. Also, we prepare the velocity model by setting Vp/Vs = 2.5 when Vp/Vs > 2.5 for comparing propagation velocities of surface waves.

In the numerical simulation results, the vertical component shows weak waves with apparent velocities of 3–4 km/s ('Diving P wave 2' in Fig. S7a). These are diving P waves excited by multiple water reverberations, and can also be observed in the horizontal component. In the water layer, near-vertically ('Diving P wave 1') and obliquely (in the x-z plane) propagating reverberations are dominant at smaller and greater offsets from the source, respectively (Fig. S7e). The diving P wave excited by the near-vertically propagating wave emerges in the horizontal component at shorter distances, while the diving P waves excited by the obliquely propagating waves emerge in the horizontal component at longer distances. This appearance variation is caused by the incident angle changes to the seafloor. The former wave is similar to the observed P wave that can be seen up to a distance of 6–7 km, and the latter waves may contribute to form the observed higher modes with higher apparent velocities.

References

Brocher, T. M. (2005). Empirical Relations between Elastic Wavespeeds and Density in the Earth's Crust. *Bulletin of the Seismological Society of America* 95(6), 2081–2092. https://doi:10.1785/0120050077

Clayton, R., & Engquist, B. (1977). Absorbing boundary condition for acoustic and elastic wave equations. *Bulletin of the Seismological Society of America* 67(6), 1529–1540. https://doi.org/10.1785/BSSA0670061529

Saenger, E. H., Gold, N., & Shapiro, S. A. (2000). Modeling the propagation of elastic waves using a modified finite-difference grid. *Wave Motion* 31, 77–92. https://doi.org/10.1016/S0165-2125(99)00023-2
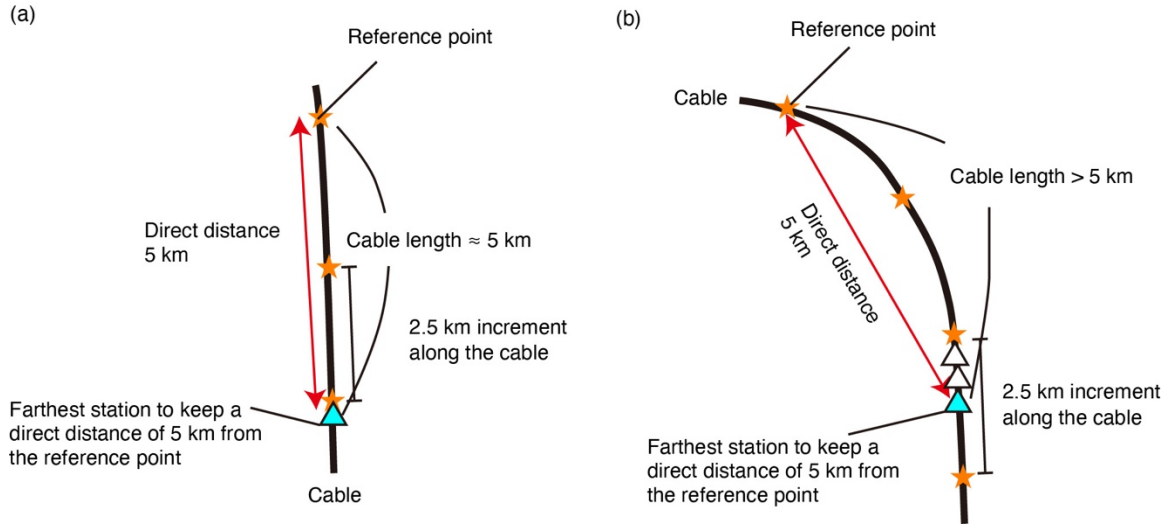
Figure S1. Sketch for the geometry among the reference points, station, and cable. (a) A linear cable with (star) the reference points and (light-blue triangle) the farthest station from the reference point. The reference point increment is 2.5 km. The distance between the farthest station and the reference point along the cable slightly exceeds 5 km. (b) A curved cable with (star) the reference points and (light-blue triangle) the farthest station. The direct distance between the farthest station and the reference point significantly along the cable exceeds 5 km. In this case, open-triangle stations that are located over a cable distance of 5 km are used, because the direct distance between the reference point and the stations is less than 5 km.
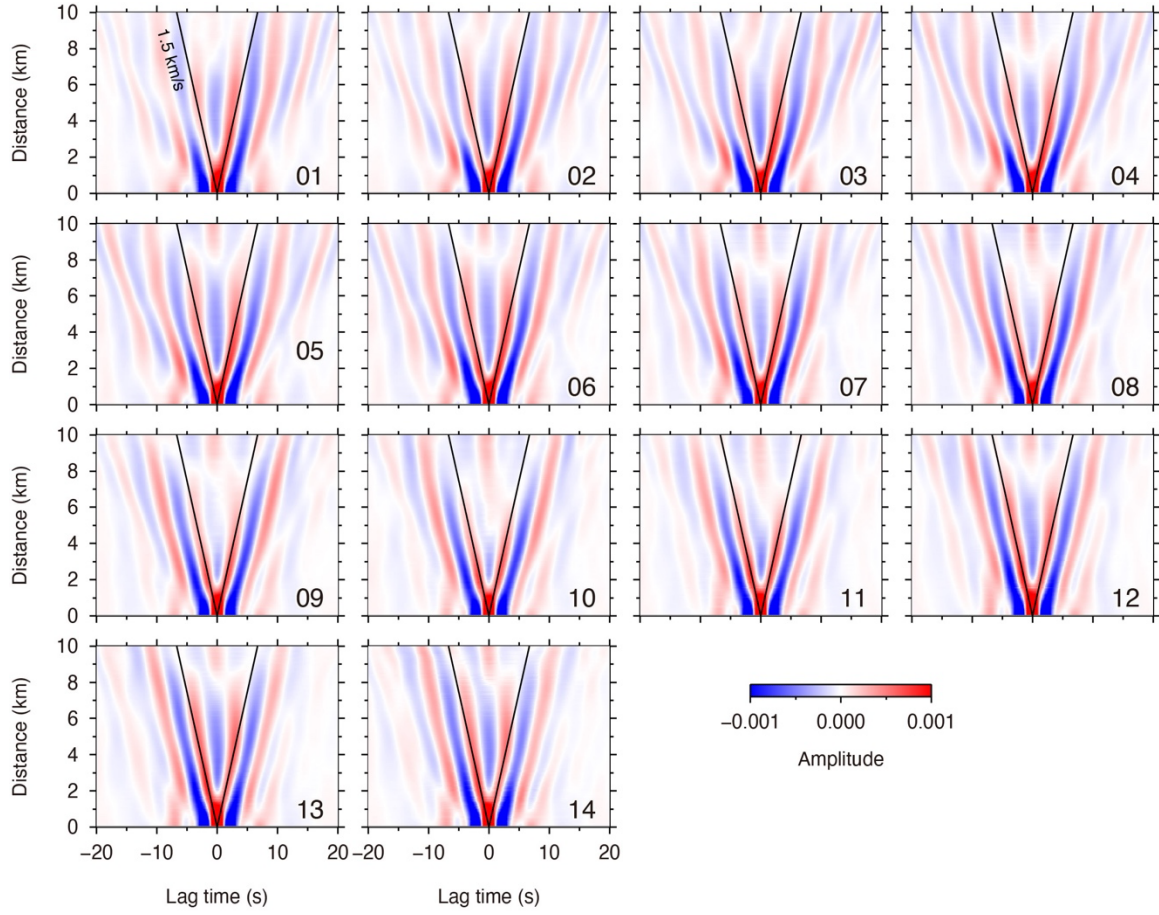
Figure S2. CCFs at 0.1–0.3 Hz for 10-km subarrays for Stage A, with the reference velocity of 1.5 km/s. The positive and negative lag times indicate the wave propagations northward and southward along the cable, respectively.
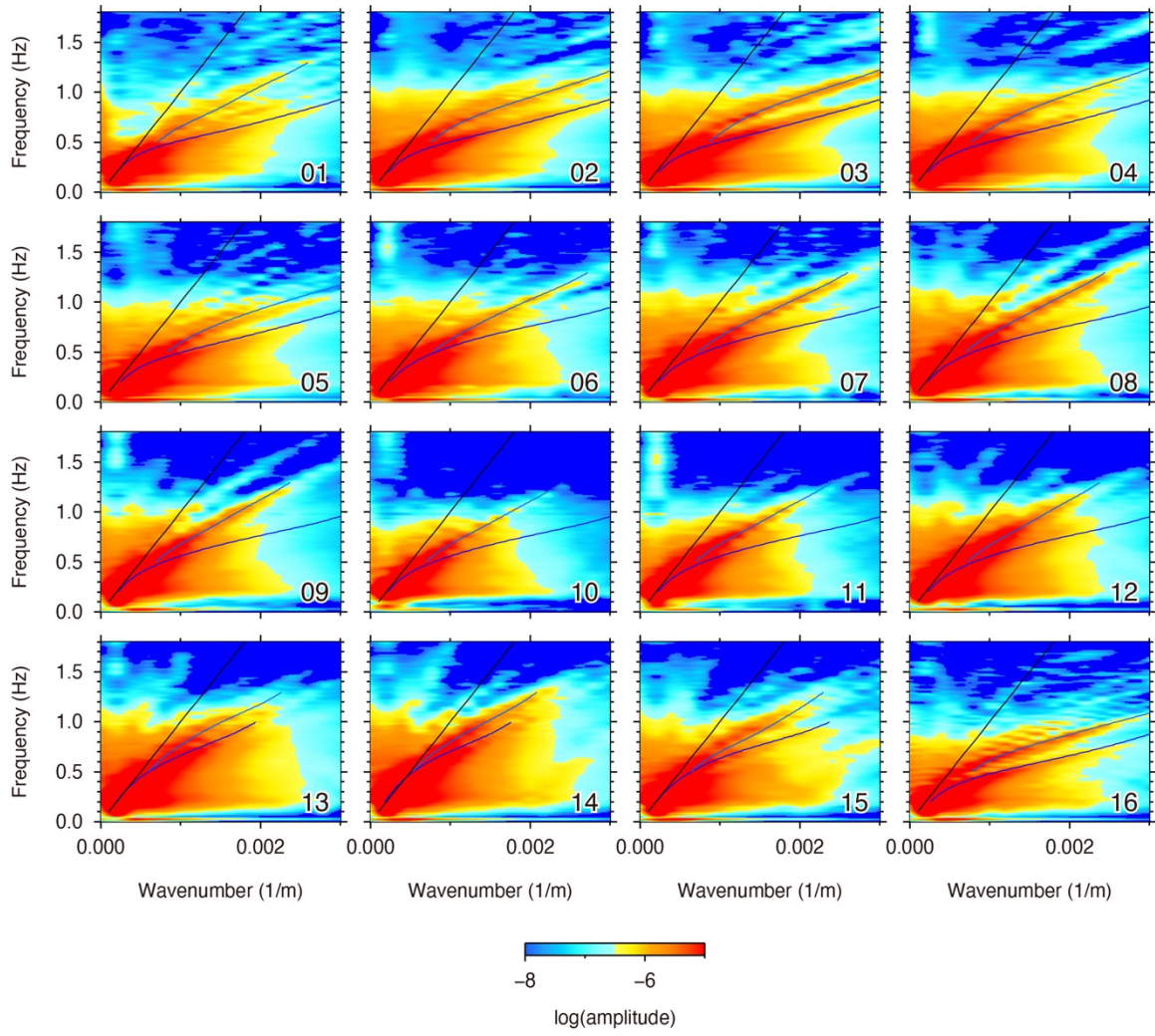
Figure S3. Same as Fig. 2b, but for subarrays 1–16.
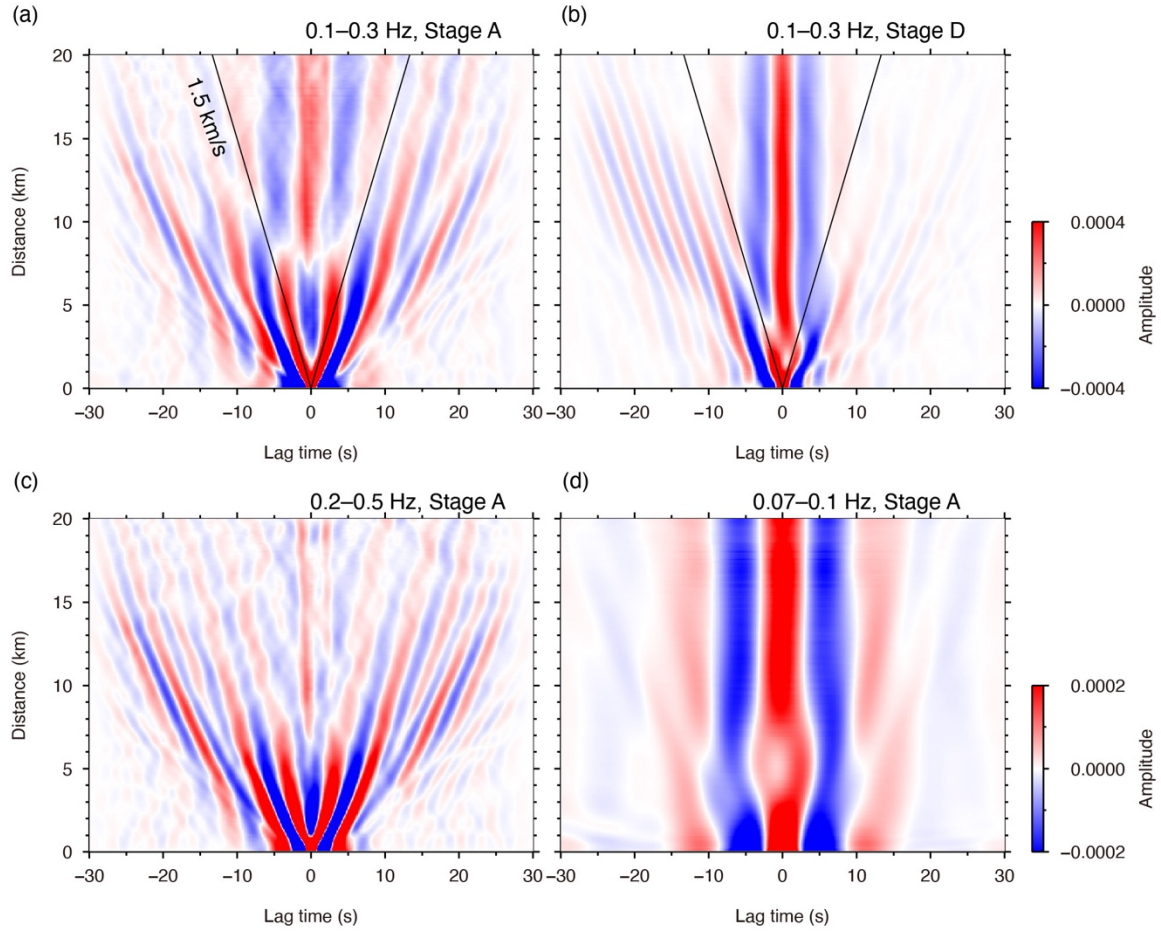
Figure S4. CCFs for different conditions. (a) Same as Fig. 2c, but the scales of the vertical and lateral axes are extended. The lines indicate the reference velocity of 1.5 km/s. (b) CCFs at 0.1–0.3 Hz for Stage D for the 20-km subarray. (c) CCFs at 0.2–0.5 Hz for Stage A for the 20-km subarray. (d) CCFs at 0.07–0.1 Hz for Stage A for the 20-km subarray.
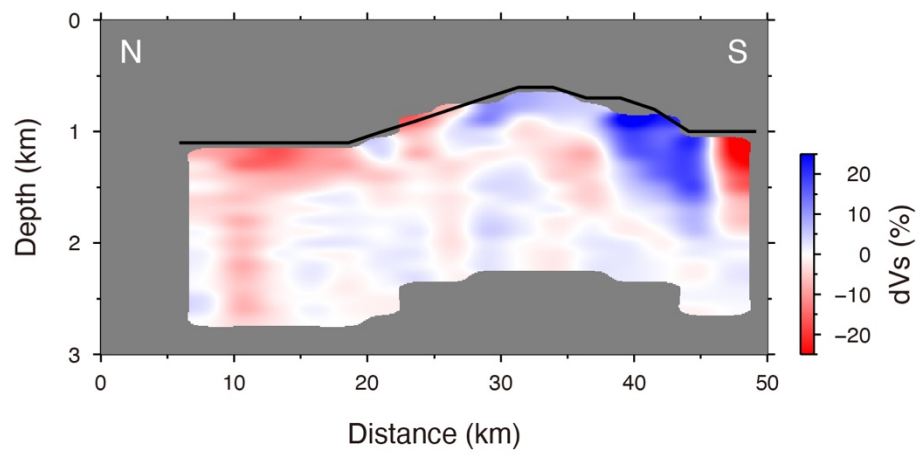
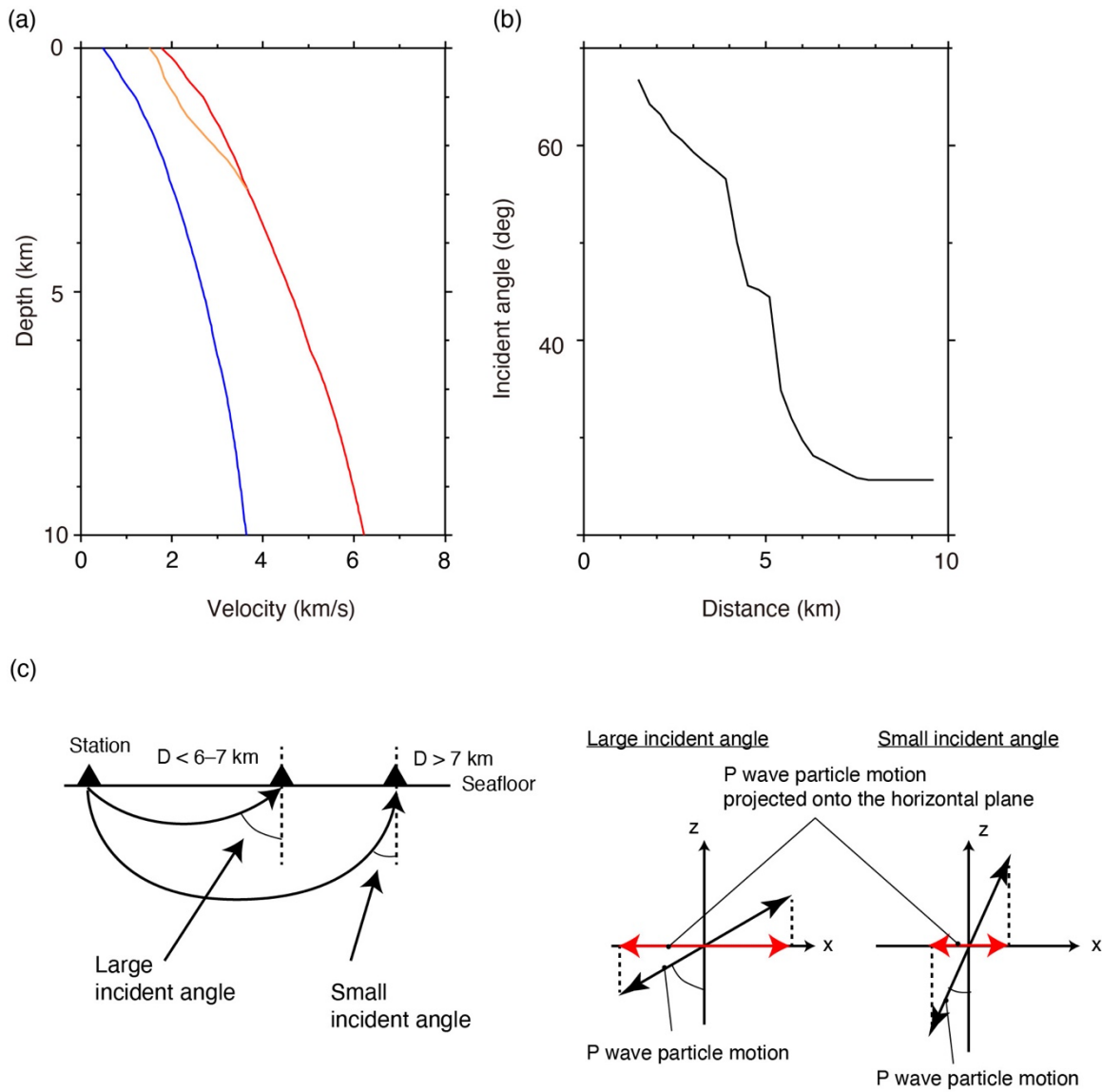**Figure S5.** Vs perturbation profiles along the cable.

Figure S6. Incident angle estimation of P waves. (a) Red and blue lines represent the reference velocity model of P and S waves. Orange line shows the reduced P-wave velocity model for calculating the theoretical travel time shown in Fig. 2d. (b) The calculated incident angle of P wave to the seafloor as a function of distance. (c) Sketch for the ray paths of P waves at short and long distances, and their horizontal particle motions according to the incident angles.
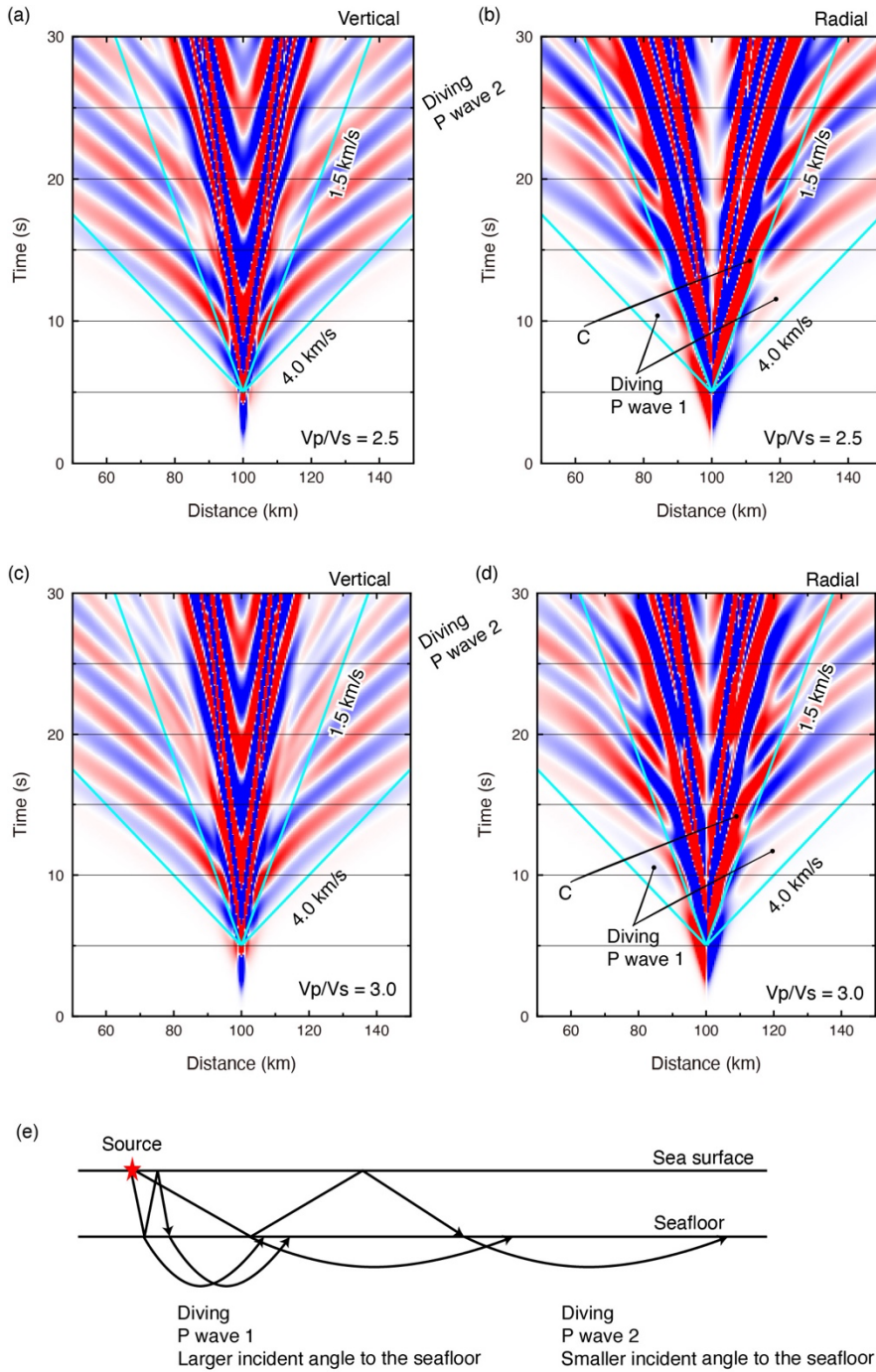
Figure S7. Numerical simulation for a single vertical force at the sea surface. (a) Synthesized waveforms in the vertical component observed at the seafloor, with reference velocities of 1.5 km/s and 4.0 km/s. The origin time is 5 s, which refers to the time of the maximum amplitude of the input Ricker wavelet. The maximum Vp/Vs was set to be 2.5. (c-d) Same as Figs. 5a and b, but for the maximum Vp/Vs of 3.0. (e) Sketch for diving *P* waves excited by water reverberations at smaller and greater offsets.
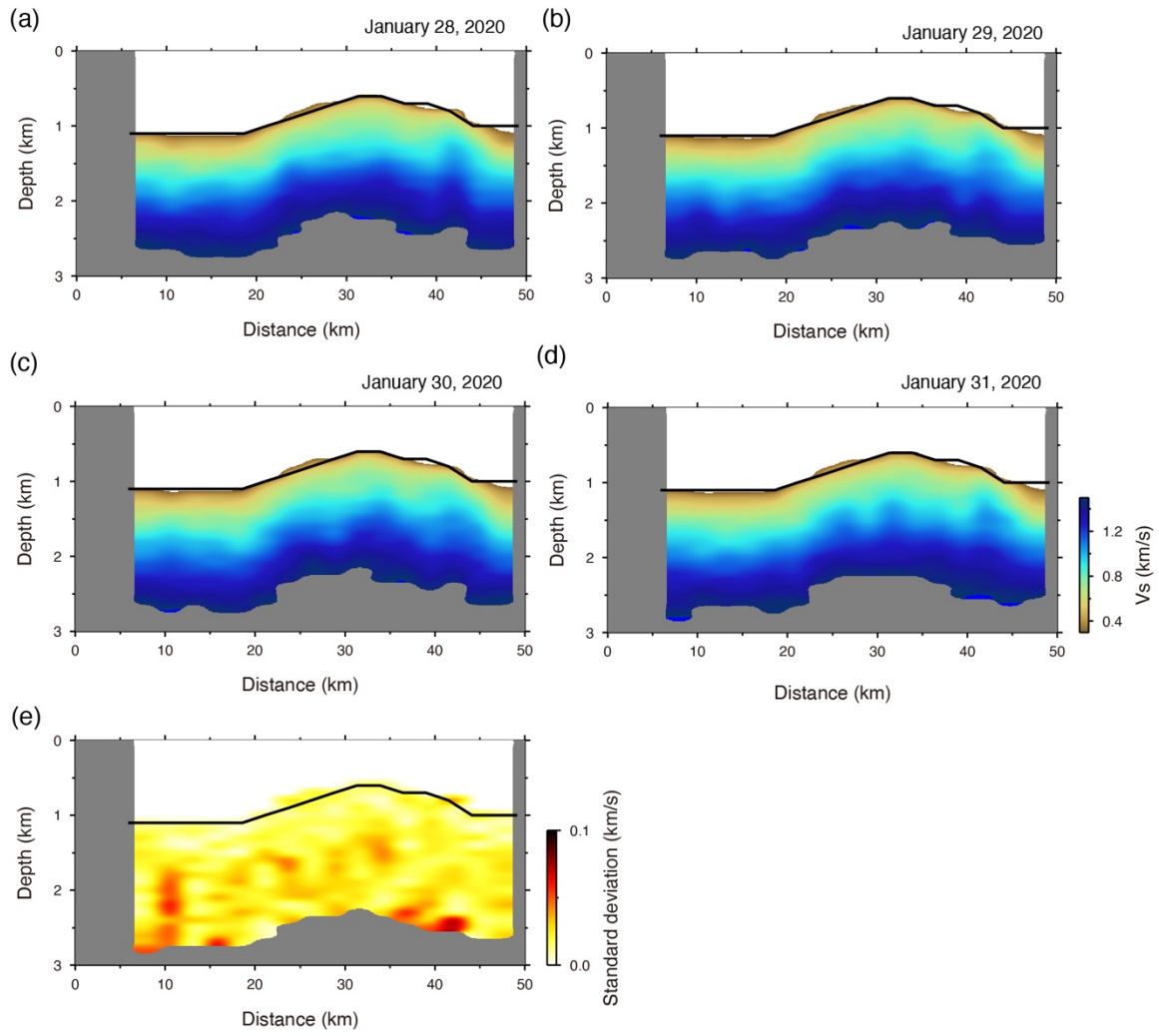
Figure S8. Same as Fig. 4a, but for (a) January 28, 2020, (b) January 29, 2020, (c) January 30, 2020, (d) January 31, 2020, and (e) the standard deviation of Vs variations of Fig. 4a and panels (a–d).

Table S1. Frequency bands used for simulated annealing and reference points.

Subarray	Fun. mode Min. freq. (Hz)	Fun. mode Max. freq. (Hz)	1st mode Min. freq. (Hz)	1st mode Max. freq. (Hz)	Reference point (km)
01	0.4	1.0	0.5	1.3	5.7
02	0.4	1.0	0.5	1.3	8.2
03	0.35	1.0	0.5	1.3	10.7
04	0.3	1.0	0.5	1.3	13.2
05	0.4	1.0	0.5	1.3	15.7
06	0.45	1.0	0.5	1.3	18.2
07	0.4	1.0	0.5	1.3	20.7
08	0.4	1.0	0.5	1.3	23.2
09	0.4	0.7	0.5	1.3	25.7
10	0.45	0.8	0.5	1.3	28.2
11	0.45	1.0	0.5	1.3	30.7
12	0.5	1.0	0.5	1.3	33.2
13	0.45	0.8	0.5	1.3	35.7
14	0.5	1.0	0.5	1.3	38.2
15	0.4	1.0	0.5	1.3	40.7
16	0.5	1.0	0.5	1.3	43.2